doi:10.1016/j.jmb.2006.07.044 J. Mol. Biol. (2006) 362, 580–593

JMB

Available online at www.sciencedirect.com

ScienceDirect

ELSEVIER

# Improving the Stability of an Antibody Variable Fragment by a Combination of Knowledge-based Approaches: Validation and Mechanisms

**Elodie Monsellier and Hugues Bedouelle***

*Unit of Molecular Prevention and Therapy of Human Diseases (CNRS FRE 2849), Institut Pasteur, 28 rue Docteur Roux 75724 Paris Cedex 15, France*

**Corresponding author*

Numerous approaches have been described to obtain variable fragments of antibodies (Fv or scFv) that are sufficiently stable for their applications. Here, we combined several knowledge-based methods to increase the stability of pre-existing scFvs by design. Firstly, the consensus sequence approach was used in a non-stringent way to predict a large basic set of potentially stabilizing mutations. These mutations were then prioritized by other methods of design, mainly the formation of additional hydrogen bonds, an increase in the hydrophilicity of solvent exposed residues, and previously described mutations in other antibodies. We validated this combined method with antibody mAbD1.3, directed against lysozyme. Fourteen potentially stabilizing mutations were designed and introduced into scFvD1.3 by site-directed mutagenesis, either individually or in combinations. We characterized the effects of the mutations on the thermodynamic stability of scFvD1.3 by experiments of unfolding with urea, monitored by spectrofluorometry, and tested the additivity of their effects by double-mutant cycles. We also quantified the individual contributions of the resistance to denaturation ($[\text{urea}]_{1/2}$) and cooperativity of unfolding ($m$) to the variations of stability and the energy of coupling between mutations by a novel approach. Most mutations (75%) were stabilizing and none was destabilizing. The progressive recombination of the mutations into the same molecule of scFvD1.3 showed that their effects were mostly additive or synergistic, provided a large overall increase in protein stability (9.1 kcal/mol), and resulted in a highly stable scFvD1.3 derivative. The mechanisms of the mutations and of their combinations involved variations in the resistance to denaturation, cooperativity of unfolding, and likely residual structures of the denatured state, which was constrained by two disulfide bonds. This combined method should be applicable to any recombinant antibody fragment, through a single step of mutagenesis.



*Keywords:* antibody engineering; consensus sequence; intrabody; protein folding; recombinant antibody

## Introduction

One of the challenges in molecular biology consists in improving the structural or functional properties of proteins at will. The antibodies constitute an excellent model to test the potential approaches to this problem because they constitute a homogeneous family of proteins and a large amount of structural and functional data is available. Improving the thermodynamic stability of their variable (Fv) or single-chain variable (scFv) fragment is also interesting from an applied point of

Abbreviations used: $V_H$ and $V_L$, variable domains of the heavy chain and light chain, respectively; Fv, variable fragment; scFv, single-chain Fv; CDR, complementary determining region; L-Gln40, amino acid residue in position 40 of the light chain; L-Q40P, mutation of L-Gln40 into L-Pro40; $\Delta\Delta G_{int}$, free energy of coupling; SE, standard error; ASA, accessible surface area.

E-mail address of the corresponding author: hbedouel@pasteur.fr

view. Such an improvement can provide an increase in their life-span for numerous applications in immunotherapy, diagnostics, proteomics and environment.[1–4] It can compensate for the loss of their two disufide bonds, one in each variable domain $V_H$ and $V_L$, and thus enable their functional expression as intrabodies in the reducing environment of the cellular cytoplasm.[5]

Many monoclonal antibodies of interest have been and are still isolated by the hybridoma technology. Others are isolated from libraries of antibody fragments that are prepared from B-cell lymphocytes of immunized animals or humans, e.g. after a vaccination or a disease.[2] These pathways of isolation may be the only possible ones for complex antigens. Therefore, the stabilization of pre-existing antibody fragments remains topical. Numerous approaches have been described to increase their stability (Table 1).[6] The knowledge-based methods are particularly simple to implement because they rely on the well-established techniques of site-directed mutagenesis and the general assumption that mutations have cumulative (generally additive) effects on stability when they are introduced simultaneously into the same molecule.

The consensus sequence approach applies to the elements of numerous families of homologous proteins and it has a firm theoretical justification.[7] In this approach, the frequencies of the amino acid residues in each position of a sequence alignment are calculated and used to deduce the consensus residue (the most frequent one). The effect of a change from a parental residue into the consensus residue on stability can be predicted by the ratio of their frequencies, as $\Delta\Delta G_{th} = -RT\ln(f_{parental}/f_{consensus})$ (see equation (1) in Materials and Methods). The values of $\Delta\Delta G_{th}$ can be used to prioritize the potentially stabilizing mutations in a member of the protein family. This method has been applied with success to variable domains of immunoglobulins,[7,8] and several other proteins.[9] A similar approach has been developed to predict stabilizing mutations in the β-turns of proteins from the frequencies of the amino acid residues in each position of the different types of turns, and applied with success to a variable domain of immunoglobulin.[10]

Here, we describe a refined method to predict stabilizing mutations in scFv fragments. It combines several methods that are knowledge-based and have been described previously (Table 1), in a multi-step algorithm. The first step uses the consensus method with a low threshold value, $\Delta\Delta G_{th} \geq 0.5$ kcal/mol. This threshold corresponds to the minimal variation of unfolding free energy that can be reliably measured with the current experimental methods; it is non-stringent and results in a large basic set of potentially stabilizing mutations. The next steps consists in prioritizing the mutations of the basic set with other methods of prediction: an increase in the propensity of forming a β-turn, the possibility of forming additional hydrogen bonds, an increase in the hydrophilicity of residues that are exposed to the solvent, or the existence of stabilizing mutations at the same position in other antibodies. The mutations of the basic set that satisfy the largest number of criteria are kept. Thus, the consensus method serves as an initial non-stringent sieve. A mutation into the consensus residue is kept only if its potential effect is corroborated by additional criteria and the different methods of prediction give coherent results.

We validated this combined method with the scFv fragment of antibody mAbD1.3, which is directed against hen egg-white lysozyme and whose unfolding can be approximated by a two-state mechanism.[11,12] We designed 14 stabilizing mutations and introduced them into scFvD1.3 by site-directed mutagenesis, either individually or in combinations. We characterized the effects of the mutations on the thermodynamic stability of scFvD1.3 by experiments of unfolding with urea, monitored by spectrofluorometry.[12] The success rate of our method was high and none of the designed mutations was destabilizing. Double-mutant thermodynamic cycles showed that the effects of the mutations were additive or synergistic in most cases.[13,14] The total increase in stability was the highest reported so far for a scFv fragment, to our knowledge.

**Table 1.** Some methods for engineering the stability of variable fragments or domains with a predefined specificity

| Method | References |
|---|---|
| Changing residues for the general consensus of antibody sequences | 7,9 |
| Engineering β-turns for increased turn-propensity | 10 |
| Creating new intramolecular hydrogen bonds | 25,52 |
| Increasing the hydrophilicity of solvent exposed residues | 25,53[a] |
| Creating inter-domain disulfide bonds | 54,55 |
| Grafting CDRs of defined specificity on a stable framework | 39,56,57 |
| Camelization | 58,59[a] |
| Fusion with a vector protein | 60–62[a],63 |
| Directed evolution by *in vitro* or *in vivo* methods | 23,64–69 |

[a] The *in vitro* stability was not measured, but the expression or activity in the cytoplasm was improved by the mutations. Only the most significant references are listed.

## Results

### Design of stabilizing mutations

We designed mutations in the scFvD1.3 fragment that could increase its thermodynamic stability, by a three-step algorithm. In a first step, we compared the amino acid sequence of scFvD1.3 with the consensus sequence of antibodies, after exclusion of the residues that belonged to the complementary determining regions (CDR) or interacted with them (Materials and Methods). Twenty-three among the 85 residues of $V_L$D1.3 that we compared, and 36/94

for $V_H$D1.3 differed from the consensus. The theoretical variation of stability $\Delta\Delta G_{th}$ was higher than 0.5 kcal/mol for 12 residues of $V_L$D1.3 and 26 residues of $V_H$D1.3 (equation (1) in Materials and Methods; Table 2, columns 1–4). These 38 changes were considered as potentially stabilizing and analyzed further.

In a second step, we used three structural criteria (Materials and Methods). (i) We identified the β-turns in the crystal structure of the FvD1.3 fragment and their types.[11,15] We then compared the propensities of the FvD1.3 and consensus residues at each position for the relevant type of turn. This comparison allowed us to predict the effect of the changes on the stability of the turns (Table 2, columns 5 and 6). (ii) We compared the crystal structures of the Fv fragments from mAbD1.3 and antibodies that were close in sequence (>85% identical residues) but had the consensus residue in the target position. This comparison showed us that eight changes potentially created an additional hydrogen bond (Table 2, columns 7 and 8). (iii) We computed the surface area that is accessible to the solvent (ASA), for each residue in the crystal structure of FvD1.3. Some residues had a hydropathy that was incompatible with their relative ASA, and a change into the consensus could resolve this incompatibility (e.g. mutation H-A62K).

In a third step, we analyzed whether similar changes of residues have been constructed in other scFvs and what is their importance for stability (e.g. L-G84A). We retained the changes of residues that satisfied the largest number of criteria (Table 2), i.e. seven single changes of residues in $V_L$D1.3 and seven in $V_H$D1.3. We grouped them in five and three primary changes, respectively, because changes that were close in the sequence could be constructed at once, and two changes, L-Q40P and L-K42Q, were simultaneously necessary to obtain the designed effect (Figure 1 and Table 3, columns 2–9).

## Construction and production of the mutants

Plasmid pMR1 codes for the wild-type scFvD1.3 fragment. The plasmids coding for the mutants of scFvD1.3 were constructed from pMR1 by one or several rounds of directed mutagenesis (Materials and Methods). The scFvD1.3 derivatives were produced in the periplasmic space of *Escherichia coli* from the mutant derivatives of pMR1 and purified by affinity chromatography through their hexa-histidine extension. The yields of production were similar for the wild-type (wt) and its mutant derivatives (mut), i.e. 0.8 to 1.0 mg of purified fragment per liter of culture at $A_{600\ nm}=2.5$. We have previously shown by mass spectrometry that the scFvD1.3 fragments have the expected molecular mass when they are produced and purified by this method.[16]

Some scFv fragments are prone to form homodimers (diabodies).[17] Therefore, we analyzed the oligomerization state of scFvD1.3 fragments by size exclusion chromatography (Figure 2). We observed that scFvD1.3, at an initial concentration of 1.8 μM, was eluted from the chromatographic column as two peaks, a major peak (~90%) with an elution volume corresponding to a monomer, and a minor peak (~10%) corresponding to a dimer. The small

**Table 2.** Design of stabilizing mutations in the wild type scFvD1.3

| Position | D1.3 | Cons | $\Delta\Delta G_{th}$ (kcal/mol) | Turn | P2/P1 | PDB | H-bonds |
|---|---|---|---|---|---|---|---|
| L-40[a] | Q | P | 2.2 | II-2 | 3.9 | 12e8 | +1, L-Q42[f] |
| L-[b] | K | Q | 0.9 | II-4 | 0.9 | 12e8 | +1, L-P40[f] |
| L-[c] | Q | K | 1.3 | | | 12e8 | +1, L-S43 |
| L-74 | K | T | 0.7 | | | 1a14 | +1, L-S20 |
| L-76 | N | S | 1.5 | I-2 | 1.2 | 12e8 | 0 |
| L-84[d] | G | A | 0.6 | | | 12e8 | 0 |
| L-85 | S | T | 1.7 | | | 1qgc | +1, L-Y87 |
| H-15 | S | G | 1.0 | II-3 | 30 | 1wej | 0 |
| H-61 | S | E | 0.7 | I-2; I-1 | 1.0; 0.5 | 1a3l | +1, H-K64[g] |
| H-62[e] | A | K | 0.9 | I-3; I-2 | 1.3; 1.1 | 1a3l | 0 |
| H-63 | L | F | 0.5 | I-4; I-3; I-1 | 1.4; 2.2; 0.7 | 1a3l | −1, H-N60 |
| H-83 | H | T | 3.8 | I-1 | 0.7 | 12e8 | +1, H-D86 |
| H-84 | T | S | 0.8 | I-2; IV-1 | 1.6; 1.2 | 12e8 | 0 |
| H-85 | D | E | 1.3 | I-3; IV-2 | 0.5; 1.2 | 1dlf | +1, H-R38 |

Column 1, residue position in Kabat's numbering. Column 2, residue in the sequence of scFvD1.3 at the position of column 1. Column 3, residue in the consensus sequence of antibodies. Column 4, $\Delta\Delta G_{th}$ upon mutation of the scFvD1.3 residue into the consensus residue, as predicted by Boltzmann's law (equation (1)). Column 5, β-turn type (in Roman numerals) and position of the residue under consideration within the β-turn (in Arabic numerals). For multiple turns, the type of each individual turn is indicated. Column 6, predicted effect of the mutation on the β-turn. P1, propensity of the scFvD1.3 residue for this position of this β-turn type; P2, propensity of the consensus residue. For multiple turns, the P2/P1 ratio for each individual turn is indicated. Column 7, PDB code for the crystal structure of an antibody with the consensus residue in the position of column 1 and more than 85% sequence identity with FvD1.3. Column 8, H-bonds established in more (+1) or in less (−1) by the consensus residue in the structure of column 7, relative to the structure of FvD1.3. The residue with which the H-bond is established, is indicated.

[a–d] Similar mutations are stabilizing in other scFvs.[8,70–73]

[e] The relative ASA of the FvD1.3 residue was not compatible with its hydropathy and the consensus residue could solve this incompatibility.

[f] Two mutations were simultaneously necessary for creating an additional H-bond.

[g] H-bond between residues $i$ and $i+3$ of a β-turn.

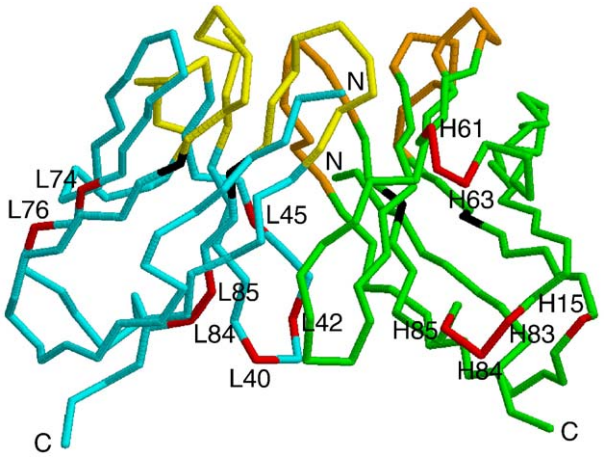


**Figure 1.** Positions of the designed mutations in the structure of FvD1.3 ($C^{\alpha}$ backbone).[11] Cyan, $V_L$; green, $V_H$; yellow, CDRs loops of $V_L$; orange, CDRs loops of $V_H$; black, Cys residues; red, single changes with their positions in $V_L$ and $V_H$. The N and C-terminal ends of each domain are indicated.

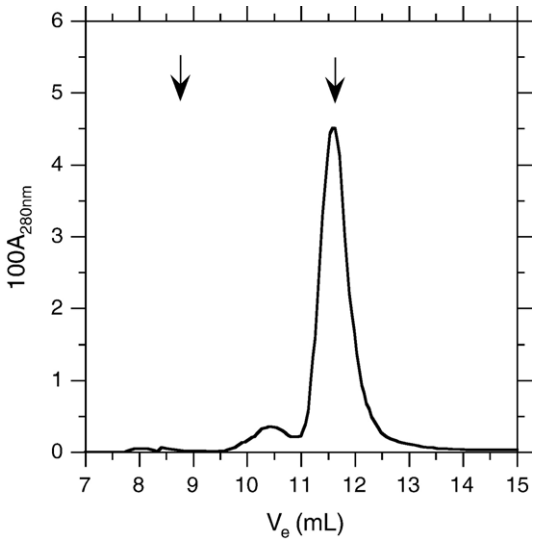


**Figure 2.** Size exclusion chromatography of the scFvD1.3(wt) fragment. The sample (1.8 μM, 200 μl) was injected on top of a Superdex 75 HR10/30 column and the chromatogram developed as described in Materials and Methods. The eluant was monitored with $A_{280\ nm}$. The elution volumes $V_e$ of bovine serum albumin (8.8 ml) and chymotrypsinogen (11.6 ml) are indicated with arrows. The major and minor peaks correspond to the scFvD1.3 monomer and dimer, respectively.

proportion of dimeric state was neglected in the experiments of denaturation with urea (see below) for three reasons. The concentration of scFvD1.3 fragment in these experiments was only 0.37 μM, i.e. fivefold lower than its concentration in the experiments of gel filtration. It was 100-fold lower than the equilibrium constants (30 μM to 300 μM) with which the homodimers of similar scFv fragments generally dissociate.[18] Finally, the monomer of the scFv fragments is generally the thermodynamically stable form.[19]

## Stability of the primary mutants

We have previously analyzed the unfolding of the scFvD1.3(wt) fragment with urea. The unfolding is reversible; it can be approximated by a two-state model and monitored with the fluorescence maximum wavelength $\lambda_{max}$. We have shown that the thermodynamic stability $\Delta G(H_2O)$, coefficient $m$ of cooperativity, and concentration $x_{1/2}$ of denaturant for half-unfolding of such a protein can be rigorously deduced from the measurement of $\lambda_{max}$ if corrective terms are applied. The corrective term on $m$ is always negligible and those on $\Delta G(H_2O)$ and $x_{1/2}$ are negligible for scFvD1.3(wt).[12] Here, we observed that the mutant derivatives of scFvD1.3 had the same behaviour as the wild-type in the unfolding experiments. In particular, the corrective terms on $\Delta G(H_2O)$, $m$ and $x_{1/2}$ were always smaller than the standard errors (SE) on these parameters and therefore neglected. These observations pertained to both primary and secondary mutants of scFvD1.3 (see below).

**Table 3.** Compositions of the scFvD1.3 mutants

| | L1 | L2 | L3 | L4 | L5 | H1 | H2 | H3 | S1 | S2 | S3 | S4 | S5 | S6 | S7 | S8 | S9 | S10 | S11 | S12 | S13 |
|---|---|---|---|---|---|---|---|---|---|---|---|---|---|---|---|---|---|---|---|---|---|
| L-Q40P | • | | | | | | | | • | | • | • | | | • | • | • | • | • | • | • |
| L-K42Q | • | | | | | | | | • | | • | • | | | • | • | • | • | • | • | • |
| L-Q45K | | • | | | | | | | | | | | | | | • | | | | • | • |
| L-K74T | | | • | | | | | | | | | | | | | • | | | | • | • |
| L-N76S | | | | • | | | | | | | | • | | • | | • | • | | • | | • |
| L-G84A | | | | | • | | | | • | | | • | | | • | • | • | • | • | • | • |
| L-S85T | | | | | • | | | | • | | | • | | | • | • | • | • | • | • | • |
| H-S15G | | | | | | • | | | | • | • | | • | • | • | | • | • | • | • | • |
| H-S61E | | | | | | | • | | | | | | • | | | | | • | • | • | • |
| H-A62K | | | | | | | • | | | | | | • | | | | | • | • | • | • |
| H-L63F | | | | | | | • | | | | | | • | | | | | • | • | • | • |
| H-H83T | | | | | | | | • | | • | | | • | • | • | | • | • | • | • | • |
| H-T84S | | | | | | | | • | | • | | | • | • | • | | • | • | • | • | • |
| H-D85E | | | | | | | | • | | • | | | • | • | • | | • | • | • | • | • |

The column headings give the names of the mutants. The first column gives the component single mutations.

Two primary mutants, L4 and H1, were as stable as scFvD1.3(wt) and the six others were more stable. These six mutants had higher values of $x_{1/2}$, higher values of $m$, or both. Three changes provided a free energy of stabilization $\Delta\Delta G(H_2O) > 2$ kcal/mol and two among them were single mutations (Table 4).

### Recombination of the stabilizing mutations

We introduced the eight primary changes progressively into a single molecule of the scFvD1.3 fragment to test whether their stabilizing effects were cumulative and obtain highly stable derivatives. The 13 secondary mutants carried from two to eight primary changes (Table 3). All the secondary mutants were more stable than the wild-type, except S3 and S4, which had the same stability (Table 4 and Figure 3). The $x_{1/2}$ values of the secondary mutants were higher than the wild-type one, without exception. The value of the cooperativity coefficient $m$ was higher than the wild-type one for six mutants (S1, S5, S8, S11, S12 and S13), close to the wild-type one for six others, and significantly lower for S3. The introduction of primary changes into the same molecule of scFvD1.3 increased the values of $\Delta G(H_2O)$ and $x_{1/2}$ incrementally. The combination of all the primary changes gave the S13 mutant with the following values of the thermodynamic parameters and of their variations: $\Delta G(H_2O) = 16.6(\pm 0.2)$ kcal/mol and $\Delta\Delta G(H_2O) = 9.1(\pm 0.4)$ kcal/mol; $m = 2.56(\pm 0.04)$ kcal/mol per M and $\Delta m = 0.8(\pm 0.1)$ kcal/mol per M; $x_{1/2} = 6.46(\pm 0.04)$ M and $\Delta x_{1/2} = 2.1(\pm 0.1)$ M (Table 4). We checked that the unfolding of the S13 mutant was reversible.

**Table 4.** Thermodynamic parameters for the unfolding of scFvD1.3(wt) and its mutant derivatives with urea at 20 °C

| Mutant | $x_{1/2}$ (M) | $m$ (kcal/mol per M) | $\Delta G(H_2O)$ (kcal/mol) | $\Delta\Delta G(H_2O)$ (kcal/mol) |
|---|---|---|---|---|
| wt | 4.4±0.1 | 1.7±0.1 | 7.4±0.4 | 0.0±0.4 |
| L1 | 4.84±0.04 | 1.7±0.2 | 8.0±0.1 | 0.6±0.4 |
| L2 | 4.28±0.07 | 2.70±0.03 | 11.6±0.3 | 4.1±0.5 |
| L3 | 4.5±0.1 | 2.3±0.1 | 10.3±0.1 | 2.9±0.4 |
| L4 | 4.40±0.02 | 1.8±0.1 | 8.1±0.5 | 0.6±0.6 |
| L5 | 4.74±0.01 | 2.1±0.1 | 9.9±0.4 | 2.5±0.5 |
| H1 | 4.85±0.02 | 1.6±0.1 | 7.6±0.4 | 0.1±0.5 |
| H2 | 4.29±0.02 | 2.1±0.2 | 9.1±0.7 | 1.6±0.8 |
| H3 | 4.64±0.03 | 1.8±0.1 | 8.3±0.6 | 0.9±0.7 |
| S1 | 4.86±0.02 | 2.7±0.2 | 13±1 | 5±1 |
| S2 | 5.12±0.03 | 2.0±0.2 | 10.3±0.9 | 3±1 |
| S3 | 5.16±0.03 | 1.43±0.08 | 7.4±0.4 | −0.1±0.5 |
| S4 | 5.50±0.03 | 1.5±0.1 | 8.2±0.5 | 0.7±0.6 |
| S5 | 5.24±0.02 | 2.1±0.1 | 11.2±0.7 | 3.8±0.7 |
| S6 | 5.50±0.02 | 1.72±0.09 | 9.5±0.5 | 2.0±0.6 |
| S7 | 5.78±0.02 | 1.8±0.1 | 10.1±0.6 | 2.7±0.7 |
| S8 | 5.34±0.02 | 2.1±0.1 | 11.1±0.6 | 3.6±0.7 |
| S9 | 6.4±0.2 | 1.55±0.08 | 9.9±0.1 | 2.4±0.4 |
| S10 | 6.11±0.03 | 1.9±0.2 | 12±1 | 4±1 |
| S11 | 6.02±0.02 | 2.4±0.2 | 14±1 | 7±1 |
| S12 | 6.44±0.02 | 2.5±0.2 | 16±1 | 9±1 |
| S13 | 6.46±0.04 | 2.56±0.04 | 16.6±0.2 | 9.1±0.4 |

The entries for $x_{1/2}$, $m$ and $\Delta G(H_2O)$ give the mean value and associated SE in two to six independent experiments (wt, and L1, L4, S9 and S13 mutants), or the value and associated SE in the curve fit (other mutants). The SE value on $\Delta\Delta G(H_2O)$ was calculated through the equation: $[SE(\Delta\Delta G)]^2 = [SE(\Delta G_{wt})]^2 + [SE(\Delta G_{mut})]^2$.

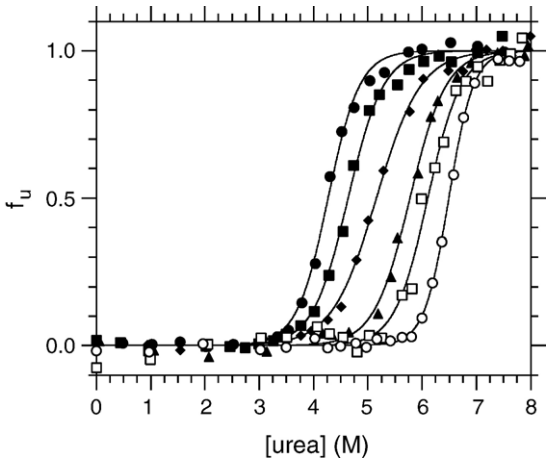


**Figure 3.** Unfolding profiles of scFvD1.3 mutants at 20 °C. Filled circles, wt; filled squares, mutant H3; diamonds, S3; triangles, S8; open squares, S10; open circles, S13. $f_d$, fraction of denatured scFvD1.3 fragment.

### Additivity of the mutations

We analyzed the 17 thermodynamic cycles of double mutants that resulted from the incremental introduction of changes into the scFvD1.3 fragment, to test the additivity of the mutational effects. We classified the couples of changes according to the free energy of coupling $\Delta\Delta G_{int}$ between them (equation (12); Table 5). The changes had synergistic effects in seven cases (40%; $\Delta\Delta G_{int}(H_2O) > 0$) and additive effects in six cases (35%; $\Delta\Delta G_{int}(H_2O) = 0$). In contrast, the second change had an antagonistic effect on the first change in three cases (17%; $\Delta\Delta G_{int}(H_2O) < 0$). The value of $\Delta\Delta G_{int}(H_2O)$ varied between −6 and +3 kcal/mol.

### Functionality of the mutant scFvD1.3 fragments

We measured and compared the rates of interaction between either scFvD1.3(wt) or scFvD1.3(S13) and lysozyme by Biacore to check whether the changes of residues modified the functionality of scFvD1.3 (Table 6). A simple model of interaction could be fitted to the profiles of association and dissociation between scFvD1.3(wt) and lysozyme. The corresponding values of the association and dissociation rate constants $k_{on}$ and $k_{off}$, and of the equilibrium dissociation constant $K_D' = k_{off}/k_{on}$ at the interface between the solid and liquid phases were consistent with those reported.[16,20,21] A simple model of interaction could not be fitted satisfactorily to the profiles for scFvD1.3(S13) ($\chi^2 = 5.1 \pm 0.6$). The most satisfying model involved a conformational change of the antibody after binding of the antigen ($\chi^2 = 0.67 \pm 0.07$). The resulting values of $K_D'$ were equal to 10(±1) nM for scFvD1.3(wt) and 13(±1) nM for scFvD1.3(S13). Thus, the mutations did not change the affinity of scFvD1.3 for its

**Table 5.** Double-mutant cycles and free energies of coupling at 20 °C in $H_2O$

| A | B | A+B | $\Delta\Delta G$(A)+ $\Delta\Delta G$(B) (kcal/mol) | $\Delta\Delta G$(A+B) (kcal/mol) | $\Delta\Delta G_{int}$ (kcal/mol) | Effect |
|---|---|---|---|---|---|---|
| L5 | L1 | S1 | 3.0±0.6 | 5±1 | 2±1 | syn |
| H3 | H1 | S2 | 1.0±0.9 | 3±1 | 2±1 | syn |
| L1 | H1 | S3 | 0.7±0.6 | −0.1±0.5 | −0.7±0.8 | n. a. |
| S1 | L4 | S4 | 6±1 | 0.7±0.6 | −5±1 | ant |
| S2 | H2 | S5 | 4±1 | 3.8±0.7 | −1±1 | add |
| S2 | L4 | S6 | 3±1 | 2.0±0.6 | −1±1 | add |
| S1 | S2 | S7 | 8±1 | 2.7±0.7 | −6±2 | ant |
| S7 | L4 | S9 | 3.3±0.9 | 2.4±0.4 | −1±1 | add |
| S2 | S4 | S9 | 3±1 | 2.4±0.4 | −1±1 | add |
| S1 | S5 | S10 | 9±1 | 4±1 | −5±2 | ant |
| S7 | H2 | S10 | 4±1 | 4±1 | 0±2 | add |
| S9 | H2 | S11 | 4.1±0.9 | 7±1 | 3±1 | syn |
| H2* | L4 | S11 | 1±1 | 4±1 | 3±2 | syn |
| S5 | S4 | S11 | 4±1 | 7±1 | 3±1 | syn |
| S10 | L4 | S11 | 5±1 | 7±1 | 2±2 | syn |
| S5 | S8 | S13 | 7±1 | 9.1±0.4 | 2±1 | syn |
| S12 | L4 | S13 | 9±1 | 9.1±0.4 | 0±1 | add |

Columns 1–3, changes A, B and A+B in scFvD1.3, with $\Delta\Delta G(A) > \Delta\Delta G(B)$. All the changes were considered in the wild-type background, except H2* which was considered in the S7 background. Column 6, free energy of coupling between changes A and B, as defined by $\Delta\Delta G_{int} = \Delta\Delta G(A+B) - \Delta\Delta G(A) - \Delta\Delta G(B)$. Column 7, effect of B on A. The classification is according to Mildvan *et al.*[14]: antagonistic (ant), $\Delta\Delta G_{int} < 0$; additive (add), $\Delta\Delta G_{int} = 0$; synergistic (syn), $0 < \Delta\Delta G_{int}$. The $\Delta\Delta G(A+B)$ and associated SE values were taken from Table 4. The SE values on $\Delta\Delta G(A) + \Delta\Delta G(B)$ and $\Delta\Delta G_{int}$ were calculated through the formulae $[SE(\Delta\Delta G(A) + \Delta\Delta G(B))]^2 = [SE(\Delta\Delta G(A))]^2 + [SE(\Delta\Delta G(B))]^2$, and $[SE(\Delta\Delta G_{int})]^2 = [SE(\Delta\Delta G(A))]^2 + [SE(\Delta\Delta G(B))]^2 + [SE(\Delta\Delta G(A+B))]^2$, respectively. n. a., not applicable.

antigen appreciably, although the precise mechanisms of binding might be different.

### Expression in the bacterial cytoplasm

We analyzed whether the higher thermodynamic stability of scFvD1.3(S13), relative to scFvD1.3(wt), translated into a higher level of production in a soluble and functional state within the cytoplasm of *E. coli* strains. The signal sequences of the encoding genes were deleted by genetic engineering of plasmids pMR1(S13) and pMR1(wt). The resulting plasmids, pEM1(S13) and pEM1(wt), respectively, were introduced into the HB2151 and Origami strains for cytoplasmic productions (Materials and Methods). The cytoplasms of the Origami strains have lower reducing potentials than that of the wild type *E. coli* strain.[22] Soluble and insoluble cellular fractions were prepared from cultures of the recombinant strains. The presence of scFvD1.3 fragments in these fractions was analyzed by Western experiments and revealed with an antibody directed against their hexa-histidine tag. scFvD1.3(wt) was undetectable in the soluble fraction of strain HB2151(pEM1(wt)). In contrast, a significant proportion of the scFvD1.3(S13) polypeptide was present in the soluble fraction of strain HB2151 (pEM1(S13)) (Table 7). The recombinant Origami strains were highly unstable. Their use did not significantly increase the level of scFvD1.3 production in the soluble fraction and this level varied widely from clone to clone. This erratic variation prevented reliable comparisons. We also tested the ability of the cellular fractions to bind immobilized lysozyme in an indirect ELISA. We detected a specific signal in the soluble fractions of both HB2151 (pEM1(S13)) and HB2151(pEM1(wt)). However, the binding activity was 20-fold higher in the S13 fraction than in the wild-type one (Table 7).

**Table 6.** Parameters for the interaction between scFvD1.3 derivatives and lysozyme at 20 °C

| Parameter | scFvD1.3(wt) | scFvD1.3(S13) |
|---|---|---|
| $k_{on1}$ ($10^5$ $M^{-1}$ $s^{-1}$) | 3.6±0.2 | 3.5±0.2 |
| $k_{off1}$ ($10^{-3}$ $s^{-1}$) | 3.8±0.3 | 16.5±0.9 |
| $k_{on2}$ ($10^{-3}$ $s^{-1}$) | n. a. | 5.2±0.8 |
| $k_{off2}$ ($10^{-3}$ $s^{-1}$) | n. a. | 2.0±0.6 |
| $K'_D$ (nM) | 10±1 | 13±1 |

Each entry gives the mean value and associated SE in at least three independent experiments. The value of $K'_D$ was calculated as follows: $K'_D = k_{off1}/k_{on1}$ for scFvD1.3(wt) (simple model); $K'_D = (k_{off1}k_{off2})/[k_{on1}(k_{on2}+k_{off2})]$ for scFvD1.3(S13) (induced fit model). n. a., not applicable.

## Discussion

### Validity of the experimental method

The profiles of unfolding with urea were cooperative and showed only one visible transition for the wild-type scFvD1.3(wt) and its 21 mutant derivatives, when monitored with the wavelength $\lambda_{max}$. These profiles were approximated satisfactorily by the equations of a two-state mechanism of unfolding (Materials and Methods; Figure 3). They did not enable one to define the characteristic parameters of an intermediate state in a three-state mechanism. In a previous study, we reviewed the experimental evidence showing that scFvD1.3(wt) unfolds according to a two-state mechanism.[12] The results of the present study were consistent with these data. If a poorly populated intermediate of unfolding existed, in which one of the two variable domains were folded and the other one unfolded, the stabilization of the folded domain by mutations should stabilize the intermediate, increase its concentration, and result either in an additional transition or at least in a

**Table 7.** Cytoplasmic expression of scFvD1.3(wt) and scFvD1.3(S13) at 24 °C

| Property | scFvD1.3(wt) | scFvD1.3(S13) |
|---|---|---|
| Soluble (%) | 0.2±0.1 | 4.3±0.6 |
| Insoluble (%) | 99.8±0.1 | 95.7±0.6 |
| $A_{405\ nm}$ | 0.024±0.002 | 0.61±0.02 |

Rows 1 and 2, fractions of the scFvD1.3 protein in a soluble or insoluble state, respectively, relative to the total amount produced and measured by densitometry of a Western blot. Row 3, signal measured in an ELISA assay, performed on soluble fractions of the producing cells, after a tenfold dilution. Each entry gives the mean value and associated SE in three independent experiments (rows 1 and 2), or three replicates of the same experiment (row 3).

decrease of the apparent value of the cooperativity coefficient $m$.[6,12] These predictions were not fulfilled by the scFvD1.3 mutants that had stabilizing mutations within only one domain (Tables 3 and 4).

### Obtaining of a highly stable scFv

We designed 14 potentially stabilizing mutations in the scFvD1.3 fragment. Among the eight primary mutants that included these mutations, six were more stable than the wild-type and two, H1 and L4, were as stable. Moreover, the changes that corresponded to H1 and L4, had additive or synergistic effects in the context of some other mutants (Table 5). Two point mutations, L3=L-K74T and L2=L-Q45K, were especially stabilizing ($\Delta\Delta G$=2.9 and 4.1 kcal/mol, respectively). Our success rate was thus >75% and no mutant was less stable than the wild-type.

scFvD1.3(wt) has an average stability for an scFv fragment, $\Delta G(H_2O)$=7.4(±0.1) kcal/mol.[12] The recombination of the designed mutations increased its stability in a cumulative process (Figure 3 and Table 4; see below). We thus obtained the scFvD1.3 (S13) derivative whose thermodynamic stability was particularly high, $\Delta G(H_2O)$=16.6(±0.2) kcal/mol. Other authors have obtained scFv derivatives with similar stabilities previously, but they started from parental scFv fragments with higher stabilities than scFvD1.3(wt), or used a succession of different methods.[23–25] The improvement in stability that we obtained for scFvD1.3, $\Delta\Delta G(H_2O)$=9.1(±0.4) kcal/mol, is the highest that has been obtained so far by a single method, to our knowledge.

### Classification of the mutations

We decomposed the variation in stability $\Delta\Delta G(H_2O)$, when going from the wild-type scFvD1.3(wt) to a mutant scFvD1.3(mut), according to three terms: (i) the contribution $m$(wt)$\Delta x_{1/2}$(mut) of the variation in parameter $x_{1/2}$; (ii) the contribution $x_{1/2}$(wt)$\Delta m$(mut) of the variation in the coefficient of cooperativity $m$; and (iii) a remainder $R$(mut), which corresponds to the mixed effect $\Delta x_{1/2}$(mut)$\Delta m$(mut), constitutes a variation of higher order, and is often negligible relative to the first two terms (equation (10); Figure 4).

The scFvD1.3 mutant derivatives could be distributed in four classes, according to the respective contributions of $\Delta x_{1/2}$ and $\Delta m$. Class 1 contained the primary changes L2, L3 and H2, for which $\Delta m$ contributed wholly to the improvement in stability. Class 2 contained the secondary changes S6 and S7, for which $\Delta x_{1/2}$ contributed wholly to the improvement. Class 3 contained changes for which both $\Delta x_{1/2}$ and $\Delta m$ contributed positively to the improvement (L5, S1, S2, S5, S8, S10, S11, S12, S13); the two contributions were approximately equal in many cases, including scFvD1.3(S13). Finally, class 4 contained the changes for which a destabilizing effect of $\Delta m$ decreased (L1 and S9) or even canceled (H1, S3 and S4) a stabilizing effect of $\Delta x_{1/2}$.

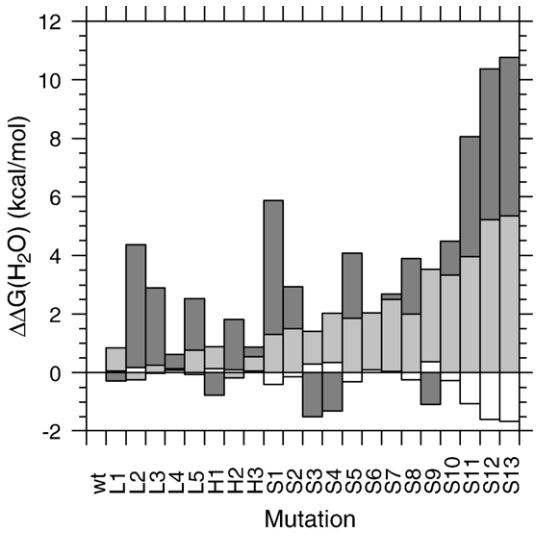


**Figure 4.** Respective contributions of $\Delta m$ and $\Delta x_{1/2}$ to the value of $\Delta\Delta G(H_2O)$ for each scFvD1.3 derivative. Dark grey, $x_{1/2}$(wt)$\Delta m$ (contribution of $\Delta m$); light grey, $m$(wt)$\Delta x_{1/2}$ (contribution of $\Delta x_{1/2}$); white, remainder $R$ (see equation (10)).

This classification showed that the stabilization of scFvD1.3 resulted from diverse mechanisms, involving an increase in $x_{1/2}$ or $m$ or both parameters. In particular, our results showed that the increase in $m$ was an important mechanism of stabilization. Parameter $x_{1/2}$ was clearly insufficient to describe the variations in stability. Thus, our results stressed the importance of having a quantitative method at one's disposal to measure the thermodynamic stability of scFv fragments.

### Molecular mechanisms of stabilization

The coefficient of cooperativity $m$ is related to the difference in the interactions that a protein makes with the denaturant in its folded and denatured states.[26] The experimental values of $m$, for a representative set of proteins, are proportional to the theoretical maximal area of surface that is exposed to the solvent on protein unfolding, empirically corrected for the effects of disulfide bonds.[27] However, both theory and experiment show that the denatured state of proteins is not fully unfolded and possess residual structures in physiological or even denaturing conditions.[28–30] Moreover, disulfide bridges favor the formation of such residual structures.[31,32]

The scFvD1.3(wt) fragment has an experimental value of $m$ which is smaller by 35% than the predicted value (1.7 *versus* 2.8 kcal/mol per M).[12] This difference suggests the existence of residual structures in the denatured state of scFvD1.3(wt) and its two disulfide bonds could favor them. The variations of $m$ that we observed here for some mutations ($-0.2 < \Delta m < 1.0$ kcal/mol per M; Table 4), were incompatible with proportionate changes in the folded state of scFvD1.3, as observed for other proteins.[29] The positive variations of $m$ could

correspond to the destruction of residual structures, a more extended conformation and a larger area of exposure to the solvent in the denatured state of the mutant scFvD1.3 fragments (compare equations (9) and (10)). Under this assumption, changes L2, S1 and S13 would fully destroy these residual structures since the corresponding mutant scFvD1.3 fragments had $m$ values close to the theoretical value (2.70(±0.03), 2.7(±0.2) and 2.56(±0.04) kcal/mol per M, respectively).

## Context effects

Mutations of residues that are not in direct contact, generally have additive effects on protein stability.[33,34] This general rule has been observed for variable domains of antibodies in particular.[25,35] The additivity or deviation from additivity (also called coupling) between two mutations or groups of mutations can be measured by thermodynamic cycles of double-mutants.[13,14,34] We constructed 17 such cycles, involving 15 different groups of mutations, to analyze this additivity in scFvD1.3 (Table 5). Seven cycles revealed synergistic effects of the two mutations or groups of mutations on stability, six showed additive effects, and three showed antagonistic effects. Thus, the association of mutations or groups of mutations was beneficial in 13/17 cases. The synergistic effects could occur between mutations that were nearby and in the same domain (e.g. S1 = L5 + L1), but also between mutations of $V_H$ and mutations of $V_L$ (e.g. S11 = S5 + S4). The same primary mutation could have different effects (additive, synergistic or antagonistic) according to the context (e.g. L4 and H2).

Some values of the coupling energy were large ($-6 < \Delta\Delta G_{int}(H_2O) < +3$ kcal/mol; Table 5). To analyze the mechanisms of additivity and its deviations, we decomposed the value of the coupling energy $\Delta\Delta G_{int}(H_2O)$ into a contribution $m(\text{wt})\Delta x_{1/2,int}(\text{mut}_1, \text{mut}_2)$ of the coupling between the $x_{1/2}$ values, a contribution $x_{1/2}(\text{wt})\Delta m_{int}(\text{mut}_1, \text{mut}_2)$ of the coupling between the $m$ values, and a remainder $R_{int}(\text{mut}_1, \text{mut}_2)$ which is of higher order and generally negligible (equation (15); Figure 5). This analysis revealed that globally additive effects of mutations on the stability of scFvD1.3 resulted from a positive (synergistic) contribution of $\Delta x_{1/2,int}$ combined with a negative (antagonistic) contribution of $\Delta m_{int}$ to the coupling energy in most cases, e.g. S9 = S7 + L4. Globally synergistic effects resulted from a strong positive contribution of $\Delta m_{int}$ in most cases, e.g. S1, S2 and S11.

The synergistic or antagonistic effects between mutations that were distant in the crystal structure of scFvD1.3 and the different effects of some mutations according to the structural context were difficult to explain by direct molecular interactions in the native state. The preponderant contribution of $m$ to non-additivity in our experiments suggested that a major part of the coupling effects occurred through the structure of the denatured state. Thus, the combination of mutations in scFvD1.3 resulted in globally beneficial but complex effects on its thermodynamic stability.

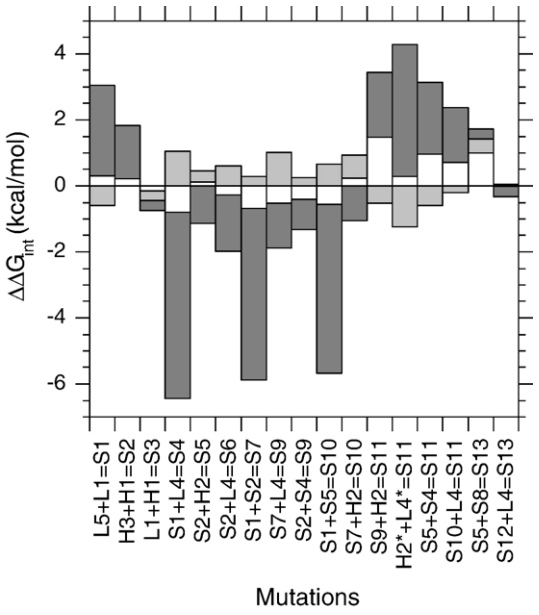


**Figure 5.** Respective contributions of $\Delta m_{int}$ and $\Delta x_{1/2,int}$ to the value of $\Delta\Delta G_{int}(H_2O)$ for each double-mutant cycle. Dark grey, $x_{1/2}(\text{wt})\Delta m_{int}$ (contribution of $\Delta m_{int}$); light grey, $m(\text{wt})\Delta x_{1/2,int}$ (contribution of $\Delta x_{1/2,int}$); white, remainder $R_{int}$ (see equation (15)).

## Reliability of the theoretical predictions

The consensus sequence approach assumes that the sequence changes have independent and additive effects.[7] We observed a good correlation between the values of $\Delta\Delta G_{th}$, calculated with equation (2), and those of $\Delta x_{1/2}$, obtained experimentally, for the single and multiple mutants of scFvD1.3 (Tables 2 and 4; $R_P = 0.95$; $p < 10^{-5}$); a significant correlation between the values of $\Delta\Delta G_{th}$ and $\Delta\Delta G(H_2O)$ ($R_P = 0.73$; $p < 0.001$); and no correlation between the values of $\Delta\Delta G_{th}$ and $\Delta m$ ($R_P = 0.22$; $p > 0.2$). Thus, the theoretical parameter $\Delta\Delta G_{th}$ predicted reliably the variation in the resistance to denaturation $x_{1/2}$ upon mutations. On the basis of these correlations, it is tempting to speculate that the evolution of the immunoglobulin framework has been more constrained by the resistance to denaturation ($x_{1/2}$) than by the cooperativity of denaturation ($m$), which is related to the existence of residual structures in the denatured state (see above). Similar correlations have been observed for the SH3 domain of protein Fyn.[36]

## General *versus* intrabody consensus

We found that the yield of production in a functional state within the reducing environment of the *E. coli* cytoplasm, was higher for the S13 mutant of scFvD1.3 than for the wild-type. Nevertheless, scFvD1.3(S13) was produced majoritarily in an insoluble state within the cytoplasm. An intra-strand

disulfide bond contributes approximately 4.5 kcal/mol to the stability of an immunoglobulin domain.[34,35] Therefore, the stability of scFvD1.3(S13) was sufficient theoretically to tolerate the absence of its two disulfide bonds in the cytoplasm, contrary to that of scFvD1.3(wt) ($\Delta G(H_2O) = 16.6$ and 7.4 kcal/mol, respectively). This difference between our experimental results and the predictions could have several causes. $\Delta x_{1/2}$ and $\Delta m$ contributed equally (5.4 kcal/mol each; Figure 4) to the strong increase in stability between the S13 mutant and the wild-type in an oxidizing medium ($\Delta\Delta G(H_2O) = 9.1$ kcal/mol). The $\Delta m$ contribution might depend on the constraints exercised on the denatured state of scFvD1.3 by the presence of the two disulfide bonds, and be lost in the reducing medium of the cytoplasm. In this hypothesis, the contribution of $\Delta x_{1/2}$ would be insufficient to compensate for the absence of the disulfide bonds. Our results showed that a high thermodynamic stability is not sufficient to obtain a scFv fragment in a functional state and with a high yield of production within the cytoplasm.

The consensus sequence of the intracellular antibodies (intrabodies) involves 124 amino acid residues in $V_H$ and $V_L$.[37] The antibodies have not been selected during evolution for solubility in the cellular cytoplasm and only a small proportion (0.5%) of them satisfies the conditions of sequence that are associated with intracellular antibodies.[38] In particular, scFvD1.3(wt) differs from the intrabody consensus sequence in 39 positions. All of the 14 mutations that we constructed in scFvD1.3, corresponded to changes into the general consensus of antibodies but only five of them corresponded to changes into the consensus of intrabodies. Therefore, the limited improvement in soluble cytoplasmic expression that we obtained with scFvD1.3 (S13), was not unexpected. However, a small increase in the soluble cytoplasmic production of an intrabody can increase its neutralizing power significantly.[39] Thus, the method of stabilization that we describe here, could contribute to improve the neutralizing activity of intrabodies obtained by other methods.

### Evaluation of the design rules

Can we rank our rules of design by their success rate? The first step of design was common to all the mutations and consisted in replacing residues of scFvD1.3 that were rare in the family of antibodies, with residues of its consensus sequence. We observed that the correlation between the values of $\Delta\Delta G_{th}$ and $\Delta\Delta G(H_2O)$ was significant (see above). The second step took three further criteria into account, based on (i) the stabilization of β-turns, (ii) the formation of additional H-bonds, and (iii) the compatibility between the hydropathy of the residues and their structural environment. The two primary changes (L4 and H1) that we designed according to the first criteria alone, did not stabilize scFvD1.3 significantly. Previous studies have reported contradictory roles of the β-turns for the stabilization of other antibody fragments or domains.[10,40] The three primary changes (L2, L3 and L5) that we designed according to the second criteria alone, were the most stabilizing. The third step took into account the changes of residues that are stabilizing in other scFv fragments, according to published data (Table 2). Together, the data reported here and in other publications suggest that the stabilizing effects of changes toward the consensus residue, are reproducible in different scFv fragments.[41] Our design rules were targeted only to the residues of the antibody framework and the most efficient ones, based on the consensus method and the formation of additional H-bonds, did not depend on its precise structure. Therefore, they should be applicable to antibody fragments whose crystal structure has not been solved. The absence of destabilizing changes suggested that it should be possible to construct the designed mutations directly into the same molecule of scFv and obtain a highly stable derivative in one step.

The consensus method has been used by other groups to increase the stability of antibody domains or fragments. In these previous studies, the mutations were chosen with very stringent criteria of sequence, i.e. the replacement of a very rare residue by a very frequent one. Only a small number of stabilizing mutations could be predicted in this way, the success rate of the predictions was comprised between 50% and 80%, and a significant proportion of the mutations was destabilizing.[9] The use of the consensus method in a non-stringent way but in combination with other criteria appears to improve its predictive power, as exemplified here.

## Conclusions

We assembled knowledge-based methods in a combined algorithm to design stabilizing mutations in scFv fragments of pre-existing antibodies. We also devised a mathematical method to decompose variations in the free energy of stabilization $\Delta G(H_2O)$ into the respective contributions of the cooperativity of unfolding ($m$) and resistance to denaturation ($[\text{denaturant}]_{1/2}$). We applied these methods to antibody mAbD1.3, directed against lysozyme. By progressively recombining 14 designed mutations into the same molecule of scFvD1.3, we obtained one of the highest increases in stability that has been reported for a scFv so far (9.1 kcal/mol). The total increase in stability was due to variations in both resistance to denaturation and cooperativity of unfolding, in equal amounts. This result suggested that some mutations acted on residual structures of the denatured state, which was constrained by two disulfide bonds. The increase in the resistance to denaturation could be predicted reliably from the sequence changes. Double-mutant cycles revealed that the effects of the mutations were additive or synergistic in most cases. The properties of the scFvD1.3 mutants showed that a very high thermodynamic stability was not a sufficient condition to obtain genuine intracellular antibodies (intrabodies).

Our combined method could be used to stabilize any scFv fragment in one step of mutagenesis. The available methods for the stabilization of antibody fragments appear to have different advantages and drawbacks, and to give complementary results. The choice of a particular method may depend on the expected result and the use of different methods may help to improve specific properties.

## Materials and Methods

### Comparison with the consensus sequence

We used Kabat's numbering for the sequences of antibodies and Chothia's definition for their complementary determining regions (CDR).[42,43] The overall consensus sequences for the variable domains $V_H$ and $V_L$ of mouse and human antibodies and the frequencies of each amino acid residue in each position were retrieved from databases†. The sequences of the scFvD1.3 fragment and consensus Fv, restricted to the framework residues, were compared and the differences of residues were compiled. The effect of a residue change on the stability of scFvD1.3 was predicted by Boltzmann's law as described:[7]

$$\Delta\Delta G_{th} = -RT\ln(f_{D1.3}/f_c) \quad (1)$$

where $f_{D1.3}$ is the frequency of the FvD1.3 residue at the corresponding position in the database of antibody sequences, $f_c$ is the frequency of the consensus residue, $R$ is the gas constant, and $T$ is temperature (K). The effect of $n$ single changes was predicted by the equation:

$$\Delta\Delta G_{th} = \sum \Delta\Delta G_{th,\,i} (i = 1, \ldots, n) \quad (2)$$

where $\Delta\Delta G_{th,i}$ is the predicted effect of the $i$th single change and the summation is over $i$.

### Structural analysis

The crystal structure of the FvD1.3 fragment has been solved at 1.8 Å resolution.[11] Its crystallographic coordinates were retrieved from the RCSB Protein Data Bank (PDB code: 1vfa). An alignment of the sequences for all the Fv fragments whose structure has been solved, was retrieved from a database‡. When FvD1.3 did not carry the consensus residue in a sequence position, its structure was compared to the structures of other Fv fragments that carried the consensus residue in that position (PDB codes: 12e8, 1a14, 1a31, 1dlf, 1dqq, 1qgc, 1qkz and 1wej). The structures were analyzed with the WHAT IF program.[44] The contacts and hydrogen bonds between residues were computed with the subprogram ANACON. We used the extended van der Waals radii, as described.[45] The solvent accessible surface area (ASA) of a residue X in a protein and its relative ASA (rASA), defined with a Gly-X-Gly tripeptide, were computed with the subprogram ACCESS and a probe radius equal to 1.4 Å. The residues were classified according to their rASA as described: exposed for 50% ≤ rASA, partially exposed for 30% ≤ rASA < 50%, and buried for rASA < 30%.[46] The following residues were considered as incompatible with a solvent exposed state: A, F, I, L, M, V, W and Y (one letter code); the following ones were considered as incompatible with a buried state: D, E, H, K, N, Q, R, S and T.[46] The β-turns were detected with the distance criterium $d(C_{\alpha,i}, C_{\alpha,i+3}) < 7.0$ Å, then classified according to the φ and ψ torsion angles of residues $i+1$ and $i+2$, where $i$ is the position of the first residue of a turn in the sequence.[15] The propensity of a residue to form a given type of turn in the structure of the FvD1.3 fragment, was compared to that of the consensus residue at the same position. When a residue was included in several overlapping turns (multiple turns), its propensities for the different turns were considered.

### Bacterial strains, plasmids and media

The *E. coli* strains HB2151,[47] RZ1032[48] and Origami (Novagen), and plasmid pMR1[16] have been described. pMR1 codes for the scFvD1.3 fragment under control of the *tet* promoter and *ompA* signal sequence from *E. coli*, in the format $NH_2$-$V_H$-$(Gly_4Ser)_3$-$V_L$-$H_6$-COOH, where $H_6$ represents a hexa-histidine tag. Buffer A was 50 mM Tris–HCl (pH 7.5), 150 mM NaCl; buffer B, 3% (w/v) bovine serum albumin (BSA, Roche) in phosphate buffer saline (PBS; Sigma); buffer C, 1% BSA in PBS.

### Recombinant DNA

The mutations were constructed by site-directed mutagenesis as described, with the single-stranded DNA of plasmid pMR1 or its derivatives as template.[48] The nucleotide sequences of the mutant genes were verified. The primary mutants of pMR1 were constructed with synthetic oligonucleotides as mutagenic primers. The secondary mutants were generally constructed by successive rounds of mutagenesis with synthetic oligonucleotides. However, the mutations of $V_L$ were recombined with those of $V_H$ by using PCR products as mutagenic primers. These PCR products were prepared as follows. A DNA fragment (829 bp) that contained the whole scFvD1.3 gene, was cut with the restriction enzymes XbaI and HindIII from the derivative of pMR1 under consideration, separated by electrophoresis, purified with the Gel extraction kit (Qiagen) and used as a template for PCR. Two synthetic oligonucleotides, hybridizing upstream and downstream of the $V_L$ gene, were phosphorylated with ATP and T4-polynucleotide kinase, and then used as PCR primers: 5′ AGTCTCCAGCCTCCCTTTC3′ and 5′CCTCCACCGA-ACGTCCGA3′. The template was amplified with Vent-polymerase (Pharmacia). The amplified DNA was purified with the QIAquick PCR purification kit (Qiagen) and used as a mutagenic primer.

Plasmid pEM1 derived from pMR1, directed the cytoplasmic expression of the scFvD1.3 fragment, and was constructed as follows. A DNA fragment (105 bp) that contained the signal sequence of the *ompA* gene and a PstI restriction site, was excised from pMR1 by digestion with the XbaI and Eco109I restriction enzymes. The large linear fragment was separated from the 105 bp fragment with a QIAquick PCR purification kit (Qiagen). A double-stranded adaptor was prepared by hybridization of the two following synthetic oligonucleotides and recombined with the large linear fragment by ligation:

5′CTAGATAACGAGGGCAAAAAATGGAAGTTAAACTA-CAGGAGTCAG3′
5′GTCCTGACTCCTGTAGTTTAACTTCCATTTTTTGCC-CTCGTTAT3′.

† www.lmb.uni-muenchen.de/groups/bs/canonical.html; www.kabatdatabase.com

‡ www.ibt.unam.mx/vir/structure/structures.html

The adaptor carried a silent mutation of the PstI site, which enabled the counter-selection of the parental pMR1 plasmid. Mutant derivatives of pEM1 were constructed from mutant derivatives of pMR1 by the same method.

### Production and purification of scFv fragments

The wild-type and mutant scFvD1.3 fragments were produced in the periplasm of strain HB2151 from plasmid pMR1 and its mutant derivatives, then purified by affinity chromatography on a column of fast-flow Ni-NTA resin (Qiagen) through their hexa-histidine extension, as described.[16] The concentration of sFvD1.3 fragment in the purified preparations was measured by absorbance spectrometry as described.[16] The wild-type scFvD1.3(wt) and mutant scFvD1.3(S13) fragments were produced in the cytoplasm of HB2151 from plasmids pEM1 and pEM1 (S13), respectively. The recombinant bacteria were grown at 24 °C until $A_{600\ nm}=0.6$, and then the expression of the scFv gene was induced during 4 h with 0.22 μg/ml of anhydrotetracycline (Sigma; 1 mg/ml stock solution in dimethyl-formamide). The bacteria were harvested by centrifugation, resuspended in one tenth volume of buffer A, kept on ice and sonicated for 5 min by pulses. The cell debris was pelleted by centrifugation during 30 min at 13,000 rpm and 4 °C. The pellet and supernatant constituted the insoluble and soluble fractions, respectively.

### Size-exclusion chromatography

The oligomeric states of the scFvD1.3 derivatives (1.8 μM, 200 μl) were analyzed by size exclusion chromatography through a Superdex 75 HR10/30 column (Amersham Biosciences), in buffer A, at room temperature, and at a flow rate of 0.5 ml/min. Bovine serum albumin ($M_r=67.2$ kDa), chymotrypsinogen ($M_r=25.0$ kDa) and acetone were used as standards.

### Stability measurements

The equilibria of unfolding at 20 °C in buffer A and the presence of urea, their monitoring with the fluorescence maximum wavelength $\lambda_{max}$, and the determination of the thermodynamic parameters corresponding to these equilibria were performed for the mutant scFvD1.3 fragments exactly as described for the wild-type.[12] In particular, we used the curvatures $b_n(0)$ and $b_d(8)$ of the fluorescence emission spectra for the proteins in 0 M and 8 M urea, respectively, to obtain rigorous values of the thermodynamic parameters, and a two-state model of unfolding that we validated for scFvD1.3(wt) previously. Three parameters are generally used to characterize such equilibria of unfolding: the difference $\Delta G(H_2O)$ of free energy between the native and denatured states of the protein in the absence of denaturant, the coefficient $m$ of cooperativity for the reaction of unfolding, and the concentration $x_{1/2}$ of denaturant (here urea) for half-advancement of this reaction. Only two of these parameters are independent, and they are linked by the general relation:

$$\Delta G(H_2O) = m x_{1/2} \tag{3}$$

### Analysis of the thermodynamic data

Let us consider a protein whose native state N and denatured state D have free energies $G_N$ and $G_D$ respectively. The free energy of denaturation, or stability, is defined by:

$$\Delta G = G_D - G_N \tag{4}$$

$\Delta G$ has a positive value since denaturation requires energy. Let us consider a wild-type protein (wt) and a mutant derivative (mut), and define the variations $\Delta\Delta G(H_2O)$, $\Delta m$ and $\Delta x_{1/2}$ by the equations:

$$\Delta G(H_2O, \text{mut}) = \Delta G(H_2O, \text{wt}) + \Delta\Delta G(H_2O, \text{mut}) \tag{5}$$

$$m(\text{mut}) = m(\text{wt}) + \Delta m(\text{mut}) \tag{6}$$

$$x_{1/2}(\text{mut}) = x_{1/2}(\text{wt}) + \Delta x_{1/2}(\text{mut}) \tag{7}$$

Developing equation (5) with equation (4) gives:

$$\Delta\Delta G(H_2O, \text{mut}) = G_D(H_2O, \text{mut}) - G_D(H_2O, \text{wt}) - [G_N(H_2O, \text{mut}) - G_N(H_2O, \text{wt})] \tag{8}$$

which can be abbreviated as:

$$\Delta\Delta G(H_2O) = \Delta G_D(H_2O) - \Delta G_N(H_2O) \tag{9}$$

where the variations are between the wild-type and mutant proteins. Thus, the variation of stability that results from a mutation depends on the effects of the mutation on both native and denatured states of the protein. If we replace $\Delta G(H_2O, \text{mut})$ and $\Delta G(H_2O, \text{wt})$ in equation (5) with their expressions in equation (3), and $m$ (mut) and $x_{1/2}$(mut) in equation (3) with their expressions in equations (6) and (7), one obtains:

$$\Delta\Delta G(H_2O) = x_{1/2}(\text{wt})\Delta m + m(\text{wt})\Delta x_{1/2} + R \tag{10}$$

i.e. $\Delta\Delta G(H_2O)$ can be decomposed into a contribution of $\Delta m$, a contribution of $\Delta x_{1/2}$ and a remainder $R$, which is of higher-order, should be negligible in most cases, and is defined by:

$$R(\text{mut}) = \Delta m(\text{mut})\Delta x_{1/2}(\text{mut}) \tag{11}$$

Note that $\Delta\Delta G(H_2O)$ is the sum of two main terms in both equations (9) and (10). How the two terms of equation (9) can be related to the two terms of equation (10) is described in Discussion.

Similarly, let us consider two mutant derivatives, $\text{mut}_1$ and $\text{mut}_2$, and the double mutant $\text{mut}_{1+2}$. By definition:

$$\Delta\Delta G(\text{H2O}, \text{mut}_{1+2}) = \Delta\Delta G(H_2O, \text{mut}_1) + \Delta\Delta G(H_2O, \text{mut}_2) + \Delta\Delta G_{int}(H_2O, \text{mut}_1, \text{mut}_2) \tag{12}$$

$$\Delta m(\text{mut}_{1+2}) = \Delta m(\text{mut}_1) + \Delta m(\text{mut}_2) + \Delta m_{int}(\text{mut}_1, \text{mut}_2) \tag{13}$$

$$\Delta x_{1/2}(\text{mut}_{1+2}) = \Delta x_{1/2}(\text{mut}_1) + \Delta x_{1/2}(\text{mut}_2) + \Delta x_{1/2,int}(\text{mut}_1, \text{mut}_2) \tag{14}$$

The coupling parameters $\Delta\Delta G_{int}(H_2O)$, $\Delta m_{int}$ and $\Delta x_{1/2,int}$ measure the deviations of $\Delta\Delta G(H_2O)$, $\Delta m$ and $\Delta x_{1/2}$ from additivity when combining two mutations or groups of mutations in the same protein molecule. By developing equation (12) with (3) and (5) (6) (7), one obtains:

$$\Delta\Delta G_{int}(H_2O) = x_{1/2}(\text{wt})\Delta m_{int} + m(\text{wt})\Delta x_{1/2,int} + R_{int} \tag{15}$$

i.e. $\Delta\Delta G_{int}(H_2O)$ can be decomposed into a contribution of $\Delta m_{int}$, a contribution of $\Delta x_{1/2,int}$ and a remainder $R_{int}$,

which is of higher order, should be negligible in most cases, and is defined by:

$$R_{\text{int}}(\text{mut}_1, \text{mut}_2) = \Delta m(\text{mut}_{1+2})\Delta x_{1/2}(\text{mut}_{1+2}) - \Delta m(\text{mut}_1)\Delta x_{1/2}(\text{mut}_1) - \Delta m(\text{mut}_2)\Delta x_{1/2}(\text{mut}_2) \quad (16)$$

### Western experiments

The Western experiments were performed as described.[49] After electro-transfer of the proteins to a nitrocellulose membrane, the scFvD1.3 fragments were revealed successively with a mouse monoclonal antibody directed against a penta-histidine (Qiagen), with a goat monoclonal antibody directed against the Fc fragment of mouse IgG and conjugated with alkaline phosphatase (Sigma), and with nitro blue tetrazolium (Sigma) and BCIP (Roche) as substrates. The membranes were scanned and the intensity of the protein bands measured by densitometry with the software Un-Scan-It gel (Silk Scientific Corporation).

### Measurement of binding activities by indirect ELISA

The relative concentrations of the scFvD1.3 fragments in soluble extracts were measured by an indirect enzyme-linked immunosorbent assay (ELISA). The wells of a microtiter plate were coated with lysozyme (10 μg/ml in buffer A) overnight at room temperature. They were then blocked with buffer B for 2 h at 37 °C. The soluble extracts were diluted tenfold in buffer C, loaded in the wells, and the plate was incubated for 1 h at room temperature. The bound molecules of scFvD1.3 were revealed as described above for the Western experiments, except that the substrate of alkaline phosphatase was *p*-nitrophenyl phosphate. The absorbance at 405 nm was both specific and linear toward the amount of scFvD1.3 in these conditions.

### Biacore

The kinetics of interaction between the scFvD1.3 fragments and lysozyme were monitored with the Biacore instrument as described.[21] Lysozyme (180 resonance units) was immobilized on a Biacore chip and the preparation of scFvD1.3 flown over lysozyme at a flow rate of 5 μl/min. The concentrations of active molecules in the preparations of scFvD1.3 were measured by the flow method as described, and used for the determination of the association rate constant $k_{\text{on}}$.[50,51]

## Acknowledgements

We thank Martial Renard for his help in an early part of the work, and Sylviane Hoos and Patrick England for their help with the Biacore. This work was supported by a grant from the French Ministry of Defense (DGA contract N° 04-34-025).

## References

1. Holliger, P. & Hudson, P. J. (2005). Engineered antibody fragments and the rise of single domains. *Nature Biotechnol.* **23**, 1126–1136.
2. Hoogenboom, H. R. (2005). Selecting and screening recombinant antibody libraries. *Nature Biotechnol.* **23**, 1105–1116.
3. Wingren, C., Steinhauer, C., Ingvarsson, J., Persson, E., Larsson, K. & Borrebaeck, C. A. (2005). Microarrays based on affinity-tagged single-chain Fv antibodies: sensitive detection of analyte in complex proteomes. *Proteomics*, **5**, 1281–1291.
4. Harris, B. (1999). Exploiting antibody-based technologies to manage environmental pollution. *Trends Biotechnol.* **17**, 290–296.
5. Stocks, M. (2005). Intrabodies as drug discovery tools and therapeutics. *Curr. Opin. Chem. Biol.* **9**, 359–365.
6. Worn, A. & Pluckthun, A. (2001). Stability engineering of antibody single-chain Fv fragments. *J. Mol. Biol.* **305**, 989–1010.
7. Steipe, B., Schiller, B., Pluckthun, A. & Steinbacher, S. (1994). Sequence statistics reliably predict stabilizing mutations in a protein domain. *J. Mol. Biol.* **240**, 188–192.
8. Ohage, E. & Steipe, B. (1999). Intrabody construction and expression. I. The critical role of VL domain stability. *J. Mol. Biol.* **291**, 1119–1128.
9. Steipe, B. (2004). Consensus-based engineering of protein stability: from intrabodies to thermostable enzymes. *Methods Enzymol.* **388**, 176–186.
10. Ohage, E. C., Graml, W., Walter, M. M., Steinbacher, S. & Steipe, B. (1997). Beta-turn propensities as paradigms for the analysis of structural motifs to engineer protein stability. *Protein Sci.* **6**, 233–241.
11. Bhat, T. N., Bentley, G. A., Boulot, G., Greene, M. I., Tello, D., Dall'Acqua, W. *et al.* (1994). Bound water molecules and conformational stabilization help mediate an antigen-antibody association. *Proc. Natl Acad. Sci. USA*, **91**, 1089–1093.
12. Monsellier, E. & Bedouelle, H. (2005). Quantitative measurement of protein stability from unfolding equilibria monitored with the fluorescence maximum wavelength. *Protein Eng. Des. Sel.* **18**, 445–456.
13. Carter, P. J., Winter, G., Wilkinson, A. J. & Fersht, A. R. (1984). The use of double mutants to detect structural changes in the active site of the tyrosyl-tRNA synthetase (*Bacillus stearothermophilus*). *Cell*, **38**, 835–840.
14. Mildvan, A. S., Weber, D. J. & Kuliopulos, A. (1992). Quantitative interpretations of double mutations of enzymes. *Arch. Biochem. Biophys.* **294**, 327–340.
15. Hutchinson, E. G. & Thornton, J. M. (1994). A revised set of potentials for beta-turn formation in proteins. *Protein Sci.* **3**, 2207–2216.
16. Renard, M., Belkadi, L., Hugo, N., England, P., Altschuh, D. & Bedouelle, H. (2002). Knowledge-based design of reagentless fluorescent biosensors from recombinant antibodies. *J. Mol. Biol.* **318**, 429–442.
17. Holliger, P., Prospero, T. & Winter, G. (1993). Diabodies: small bivalent and bispecific antibody fragments. *Proc. Natl Acad. Sci. USA*, **90**, 6444–6448.
18. Lee, Y. C., Boehm, M. K., Chester, K. A., Begent, R. H. J. & Perkins, S. J. (2002). Reversible dimer formation and stability of the anti-tumour single-chain Fv antibody MFE-23 by neutron scattering, analytical ultracentrifugation, and NMR and FT-IR spectroscopy. *J. Mol. Biol.* **320**, 107–127.
19. Arndt, K. M., Müller, K. M. & Plückthun, A. (1998). Factors influencing the dimer to monomer transition of an antibody single-chain Fv fragment. *Biochemistry*, **37**, 12918–12926.
20. England, P., Bregegere, F. & Bedouelle, H. (1997). Energetic and kinetic contributions of contact residues

of antibody D1.3 in the interaction with lysozyme. *Biochemistry*, **36**, 164–172.
21. England, P., Nageotte, R., Renard, M., Page, A. L. & Bedouelle, H. (1999). Functional characterization of the somatic hypermutation process leading to antibody D1.3, a high affinity antibody directed against lysozyme. *J. Immunol.* **162**, 2129–2136.
22. Prinz, W. A., Aslund, F., Holmgren, A. & Beckwith, J. (1997). The role of the thioredoxin and glutaredoxin pathways in reducing protein disulfide bonds in the *Escherichia coli* cytoplasm. *J. Biol. Chem.* **272**, 15661–15667.
23. Jung, S., Honegger, A. & Pluckthun, A. (1999). Selection for improved protein stability by phage display. *J. Mol. Biol.* **294**, 163–180.
24. Martineau, P. & Betton, J. M. (1999). *In vitro* folding and thermodynamic stability of an antibody fragment selected *in vivo* for high expression levels in *Escherichia coli* cytoplasm. *J. Mol. Biol.* **292**, 921–929.
25. Ewert, S., Honegger, A. & Pluckthun, A. (2003). Structure-based improvement of the biophysical properties of immunoglobulin VH domains with a generalizable approach. *Biochemistry*, **42**, 1517–1528.
26. Schellman, J. A. (1994). The thermodynamics of solvent exchange. *Biopolymers*, **34**, 1015–1026.
27. Myers, J. K., Pace, C. N. & Scholtz, J. M. (1995). Denaturant m values and heat capacity changes: relation to changes in accessible surface areas of protein unfolding. *Protein Sci.* **4**, 2138–2148.
28. Dill, K. A. & Shortle, D. (1991). Denatured states of proteins. *Annu. Rev. Biochem.* **60**, 795–825.
29. Shortle, D. (1996). The denatured state (the other half of the folding equation) and its role in protein stability. *FASEB J.* **10**, 27–34.
30. Fersht, A. R. & Daggett, V. (2002). Protein folding and unfolding at atomic resolution. *Cell*, **108**, 573–582.
31. Betz, S. F. & Pielak, G. J. (1992). Introduction of a disulfide bond into cytochrome *c* stabilizes a compact denatured state. *Biochemistry*, **31**, 12337–12344.
32. Clarke, J., Hounslow, A. M., Bond, C. J., Fersht, A. R. & Daggett, V. (2000). The effects of disulfide bonds on the denatured state of barnase. *Protein Sci.* **9**, 2394–2404.
33. Wells, J. A. (1990). Additivity of mutational effects in proteins. *Biochemistry*, **29**, 8509–8517.
34. Fersht, A. R. (1999). *Structure and Mechanism in Protein Science: A Guide to Enzyme Catalysis and Protein Folding*, W.H. Freeman, New York.
35. Frisch, C., Kolmar, H. & Fritz, H. J. (1994). A soluble immunoglobulin variable domain without a disulfide bridge: construction, accumulation in the cytoplasm of *E. coli*, purification and physicochemical characterization. *Biol. Chem. Hoppe Seyler*, **375**, 353–356.
36. Di Nardo, A. A., Larson, S. M. & Davidson, A. R. (2003). The relationship between conservation, thermodynamic stability, and function in the SH3 domain hydrophobic core. *J. Mol. Biol.* **333**, 641–655.
37. Visintin, M., Settanni, G., Maritan, A., Graziosi, S., Marks, J. D. & Cattaneo, A. (2002). The intracellular antibody capture technology (IACT): towards a consensus sequence for intracellular antibodies. *J. Mol. Biol.* **317**, 73–83.
38. Visintin, M., Quondam, M. & Cattaneo, A. (2004). The intracellular antibody capture technology: towards the high-throughput selection of functional intracellular antibodies for target validation. *Methods*, **34**, 200–214.
39. Worn, A., Auf der Maur, A., Escher, D., Honegger, A., Barberis, A. & Pluckthun, A. (2000). Correlation between *in vitro* stability and *in vivo* performance of anti-GCN4 intrabodies as cytoplasmic inhibitors. *J. Biol. Chem.* **275**, 2795–2803.
40. Niggemann, M. & Steipe, B. (2000). Exploring local and non-local interactions for protein stability by structural motif engineering. *J. Mol. Biol.* **296**, 181–195.
41. Wall, J. G. & Pluckthun, A. (1999). The hierarchy of mutations influencing the folding of antibody domains in *Escherichia coli*. *Protein Eng.* **12**, 605–611.
42. Johnson, G. & Wu, T. T. (2000). Kabat Database and its applications: 30 years after the first variability plot. *Nucl. Acids Res.* **28**, 214–218.
43. Al-Lazikani, B., Lesk, A. M. & Chothia, C. (1997). Standard conformations for the canonical structures of immunoglobulins. *J. Mol. Biol.* **273**, 927–948.
44. Vriend, G. (1990). WHAT IF: a molecular modeling and drug design program. *J. Mol. Graph.* **8**, 52–56.
45. Rondard, P. & Bedouelle, H. (1998). A mutational approach shows similar mechanisms of recognition for the isolated and integrated versions of a protein epitope. *J. Biol. Chem.* **273**, 34753–34759.
46. Chowdhury, P. S., Vasmatzis, G., Beers, R., Lee, B. & Pastan, I. (1998). Improved stability and yield of a Fv-toxin fusion protein by computer design and protein engineering of the Fv. *J. Mol. Biol.* **281**, 917–928.
47. Carter, P., Bedouelle, H. & Winter, G. (1985). Improved oligonucleotide site-directed mutagenesis using M13 vectors. *Nucl. Acids Res.* **13**, 4431–4443.
48. Kunkel, T. A., Roberts, J. D. & Zakour, R. A. (1987). Rapid and efficient site-specific mutagenesis without phenotypic selection. *Methods Enzymol.* **154**, 367–382.
49. Sambrook, J. & Russel, D. W. (2001). *Molecular Cloning, A Laboratory Manual*, 3rd edit., CSH Laboratory Press, Cold Spring Harbor, NY.
50. Richalet-Secordel, P. M., Rauffer-Bruyere, N., Christensen, L. L., Ofenloch-Haehnle, B., Seidel, C. & Van Regenmortel, M. H. (1997). Concentration measurement of unpurified proteins using biosensor technology under conditions of partial mass transport limitation. *Anal. Biochem.* **249**, 165–173.
51. Christensen, L. L. (1997). Theoretical analysis of protein concentration determination using biosensor technology under conditions of partial mass transport limitation. *Anal. Biochem.* **249**, 153–164.
52. Pokkuluri, P. R., Gu, M., Cai, X., Raffen, R., Stevens, F. J. & Schiffer, M. (2002). Factors contributing to decreased protein stability when aspartic acid residues are in beta-sheet regions. *Protein Sci.* **11**, 1687–1694.
53. Kaufmann, M., Lindner, P., Honegger, A., Blank, K., Tschopp, M., Capitani, G. *et al.* (2002). Crystal structure of the anti-His tag antibody 3D5 single-chain fragment complexed to its antigen. *J. Mol. Biol.* **318**, 135–147.
54. Glockshuber, R., Malia, M., Pfitzinger, I. & Pluckthun, A. (1990). A comparison of strategies to stabilize immunoglobulin Fv-fragments. *Biochemistry*, **29**, 1362–1367.
55. Reiter, Y., Brinkmann, U., Lee, B. & Pastan, I. (1996). Engineering antibody Fv fragments for cancer detection and therapy: disulfide-stabilized Fv fragments. *Nature Biotechnol.* **14**, 1239–1245.
56. Jung, S. & Pluckthun, A. (1997). Improving *in vivo* folding and stability of a single-chain Fv antibody fragment by loop grafting. *Protein Eng.* **10**, 959–966.
57. Donini, M., Morea, V., Desiderio, A., Padskoulov, D., Villani, M. E., Tramontano, A. & Benvenuto, E. (2003). Engineering stable cytoplasmic intrabodies with designed specificity. *J. Mol. Biol.* **330**, 323–332.

58. Davies, J. & Riechmann, L. (1996). Single antibody domains as small recognition units: design and *in vitro* antigen selection of camelized, human VH domains with improved protein stability. *Protein Eng.* **9**, 531–537.
59. Aires da Silva, F., Santa-Marta, M., Freitas-Vieira, A., Mascarenhas, P., Barahona, I., Moniz-Pereira, J., Gabuzda, D. & Goncalves, J. (2004). Camelized rabbit-derived VH single-domain intrabodies against Vif strongly neutralize HIV-1 infectivity. *J. Mol. Biol.* **340**, 525–542.
60. Bregegere, F., Schwartz, J. & Bedouelle, H. (1994). Bifunctional hybrids between the variable domains of an immunoglobulin and the maltose-binding protein of *Escherichia coli*: production, purification and antigen binding. *Protein Eng.* **7**, 271–280.
61. Bach, H., Mazor, Y., Shaky, S., Shoham-Lev, A., Berdichevsky, Y., Gutnick, D. L. & Benhar, I. (2001). *Escherichia coli* maltose-binding protein as a molecular chaperone for recombinant intracellular cytoplasmic single-chain antibodies. *J. Mol. Biol.* **312**, 79–93.
62. Zhang, Z., Li, Z. H., Wang, F., Fang, M., Yin, C. C., Zhou, Z. Y. *et al.* (2002). Overexpression of DsbC and DsbG markedly improves soluble and functional expression of single-chain Fv antibodies in *E. coli*. *Protein Expr. Purif.* **26**, 218–228.
63. Strube, R. W. & Chen, S. Y. (2004). Enhanced intracellular stability of sFv-Fc fusion intrabodies. *Methods*, **34**, 179–183.
64. Martineau, P., Jones, P. & Winter, G. (1998). Expression of an antibody fragment at high levels in the bacterial cytoplasm. *J. Mol. Biol.* **280**, 117–127.
65. Proba, K., Worn, A., Honegger, A. & Pluckthun, A. (1998). Antibody scFv fragments without disulfide bonds made by molecular evolution. *J. Mol. Biol.* **275**, 245–253.
66. Jermutus, L., Honegger, A., Schwesinger, F., Hanes, J. & Pluckthun, A. (2001). Tailoring in vitro evolution for protein affinity or stability. *Proc. Natl Acad. Sci. USA*, **98**, 75–80.
67. Jespers, L., Schon, O., Famm, K. & Winter, G. (2004). Aggregation-resistant domain antibodies selected on phage by heat denaturation. *Nature Biotechnol.* **22**, 1161–1165.
68. Graff, C. P., Chester, K., Begent, R. & Wittrup, K. D. (2004). Directed evolution of an anticarcinoembryonic antigen scFv with a 4-day monovalent dissociation half-time at 37 degrees C. *Protein Eng. Des. Sel.* **17**, 293–304.
69. Brockmann, E. C., Cooper, M., Stromsten, N., Vehniainen, M. & Saviranta, P. (2005). Selecting for antibody scFv fragments with improved stability using phage display with denaturation under reducing conditions. *J. Immunol. Methods*, **296**, 159–170.
70. Wetzel, R. (1997). Domain stability in immunoglobulin light chain deposition disorders. *Adv. Protein Chem.* **50**, 183–242.
71. Chan, W., Helms, L. R., Brooks, I., Lee, G., Ngola, S., McNulty, D. *et al.* (1996). Mutational effects on inclusion body formation in the periplasmic expression of the immunoglobulin VL domain REI. *Fold. Des.* **1**, 77–89.
72. Forsberg, G., Forsgren, M., Jaki, M., Norin, M., Sterky, C., Enhorning, A., Larsson, K., Ericsson, M. & Bjork, P. (1997). Identification of framework residues in a secreted recombinant antibody fragment that control production level and localization in *Escherichia coli*. *J. Biol. Chem.* **272**, 12430–12436.
73. Hurle, M. R., Helms, L. R., Li, L., Chan, W. & Wetzel, R. (1994). A role for destabilizing amino acid replacements in light-chain amyloidosis. *Proc. Natl Acad. Sci. USA*, **91**, 5446–5450.

***Edited by I. Wilson***

*(Received 7 May 2006; received in revised form 17 July 2006; accepted 20 July 2006)*
Available online 28 July 2006